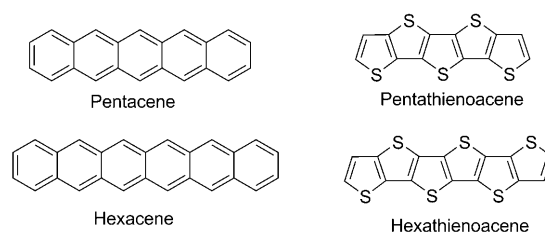


Hexathienoacene: Synthesis, Characterization, and Thin-Film Transistors

Ying Liu,^[a, b] Xiangnan Sun,^[a, b] Chong-an Di,^[a] Yunqi Liu,^{*, [a]} Chunyan Du,^[a, b] Kun Lu,^[a] Shanghai Ye,^[a, b] and Gui Yu^[a]

During the past ten years, organic thin-film transistors (OTFTs) based on organic π -conjugated molecules have attracted much attention because of many advantages in contrast to conventional silicon-based transistors, for instance, low fabrication cost, large-area manufacturing, and flexibility.^[1] Linearly fused acenes and heteroacenes have attracted considerable attention as the most viable materials for OTFTs.^[2] Pentacene, a member of the acene series of linear aromatic systems, is the current benchmark semiconductor for OTFTs. However, pentacene is unstable and degrades rapidly under ambient conditions, because it is subject to photoinduced decomposition in the 6- and 15-positions owing to π -electron localization.^[3] Hexacene, as higher polyacenes, was found to be extremely unstable in solution, presumably because of its higher reactivity toward dimerization and oxidation.^[4] The only characterization data reported to date are a combustion analysis^[5] and a UV/Vis spectrum,^[6] which has limited its proper study for applications. Oligothienoacenes (n TAs: fully fused oligothiophenes) are recognized as the thiophene analogues of acenes. The advantages of these molecules have been attributed to their unique structural features: All the sulfur atoms are positioned at the molecular periphery, facilitating multiple short intermolecular S \cdots S contacts which increase the effective dimensionality of the electronic structure, with the result that they may possess enhanced transport properties.

The charge carrier mobility in organic materials generally increases with the extension of conjugation. For example, hole mobilities of 0.12 and 3.0 cm²V⁻¹s⁻¹ have been reported for thin films of tetracene^[7] and pentacene,^[8] respectively. As for oligothienoacenes, our group has fabricated pentathienoacene (PTA) as active semiconducting layers for OTFTs with good mobility, which indicates that materials based on thiophene-fused systems are a promising class of organic materials for their use in OTFTs.^[9] Further extension of the conjugation results in hexathienoacene (HTA, a six-thiophene-fused system, Scheme 1) or other higher fused



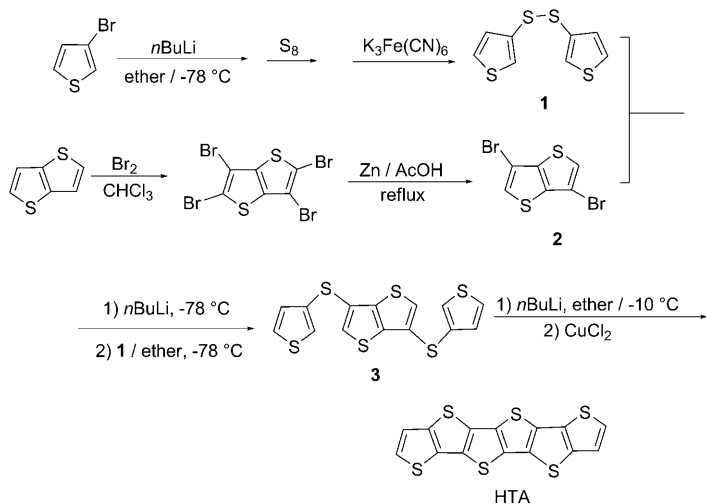
Scheme 1. Chemical structures of pentacene, pentathienoacene, hexacene, and hexathienoacene.

oligothiophenes;^[10] probably because of the lack of convenient synthetic routes, devices utilizing these oligothienoacenes have not been studied. Herein we report the synthesis, characterization, and performance of a fully fused oligothiophene HTA as a new *p*-type organic semiconductor and also compare the properties to those of PTA. Although the yield of HTA (6.0%) was a little lower, as shown in Scheme 2, the compounds bis(3-thienyl) disulfide (**1**)^[11] and 3,6-dibromothienothiophene (**2**)^[12] can be operated in a large scale to synthesize 6-bis-(thiophen-3-ylsulfanyl)-thieno[3,2-*b*]thiophene (**3**) in high yield. In this paper, on the basis of our research interests in fused thiophenes for OTFTs,^[9, 13] we tried to investigate the effects of increasing extension of the conjugation from PTA to HTA on the optical, electrochemical properties, and charge-transfer properties of organic semi-

[a] Y. Liu, X. Sun, Dr. C.-a. Di, Prof. Y. Liu, C. Du, Dr. K. Lu, S. Ye, Prof. G. Yu
Key Laboratory of Organic Solids
Institute of Chemistry
Chinese Academy of Sciences
Beijing 100190 (P.R. China)
Fax: (+86)10-62559373
E-mail: liuyq@iccas.ac.cn

[b] Y. Liu, X. Sun, C. Du, S. Ye
Graduate School of Chinese Academy of Sciences
Beijing 100039 (P.R. China)

Supporting information for this article is available on the WWW under <http://dx.doi.org/10.1002/asia.201000001>.



Scheme 2. Synthetic routes of HTA.

conductors by comparison with the density functional theory (DFT) study by Jiang and co-workers.^[14]

HTA was synthesized as shown in Scheme 2. Compounds **1**^[11] and **2**^[12] were prepared according to the literature procedures. Compound **2** was lithiated with *n*-butyllithium (*n*BuLi) in diethyl ether, and then reacted with **1** to give **3** as a white solid in 85% yield. Oxidative ring closure of **3** to obtain HTA is a vital procedure. The solution of **3** in diethyl ether lithiated with *n*BuLi at -10°C was added to a vigorously stirred suspension of anhydrous copper chloride (CuCl_2) at 0°C in diethyl ether, which was employed to afford the final product HTA in the yield of 6.0%. After purification by thermal gradient zone purification processes, the product is a yellow solid and slightly soluble in hot toluene or chlorobenzene. Its chemical structure was determined by high-resolution mass spectrometry (HRMS) and elemental analysis. The thermal property was measured by thermal gravimetric analysis (TGA) performed under nitrogen with the onset of weight loss at well over 300°C , demonstrating a high thermal stability.

The optical and electrochemical data of PTA and HTA are summarized in Table 1. The UV/Vis absorption spectroscopy data for HTA were measured in THF solution with many absorption peaks at 312, 324, 360, and 380 nm and the emission peak at 416 nm (Figure 1). As expected, the maximum intensity wavelength of HTA is red-shifted compared to that of PTA in both absorption and emission (listed in

Table 1. Optical and electrochemical properties of PTA and HTA.

Cmpd	$\lambda_{\text{abs}}^{[\text{a}]}$ [nm]	$\lambda_{\text{em}}^{[\text{a}]}$ [nm]	$\lambda_{\text{abs}}^{[\text{b}]}$ [nm]	$E_{\text{g}}^{[\text{c}]}$ [eV]	$E_{\text{HOMO}}^{[\text{d}]}$ [eV]	$\mu_{\text{TFT}}^{[\text{e}]}$ [$\text{cm}^2 \text{V}^{-1} \text{s}^{-1}$]
PTA ^[\text{e}]	358	344	342	3.20	3.77 ^[\text{f}]	-5.33 $-5.30^{[\text{f}]}$ 2.2×10^{-3} $0.55^{[\text{f}]}$
HTA	380	416	352	3.10	3.53 ^[\text{f}]	-5.06 $-5.20^{[\text{f}]}$ 4.3×10^{-3} $0.48^{[\text{f}]}$

[a] Measurements performed in a dilute THF solution (ca. 10^{-5}M). [b] Measurements performed on vacuum-deposited film. [c] Estimated from the onset of absorption in a dilute solution ($E_{\text{g}} = 1240/\lambda_{\text{onset}}$ eV). [d] Calculated using the empirical equation: $E_{\text{HOMO}} = -(4.40 + E_{\text{ox}})$ eV. [e] All the data of PTA are cited in reference [9]. [f] Density functional theory (DFT) calculations; see reference [14].

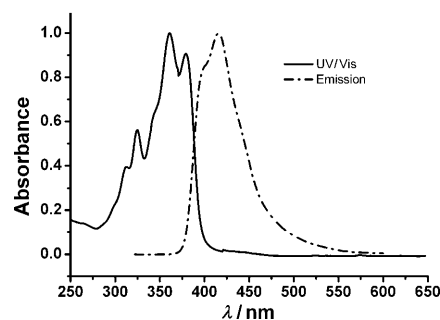


Figure 1. Normalized UV/Vis absorption spectra and emission spectra in THF solution.

Table 1), which indicates that introduction of a thiophene unit leads to extended conjugation and decreased HOMO–LUMO gap. A HOMO–LUMO gap of 3.10 eV was estimated from the absorption edge of 400 nm in dilute THF solution, which is close in energy to that of PTA (3.20 eV). For the vacuum-deposited thin-film absorption spectrum of HTA, the maximum absorption appears at 352 nm, slightly blue-shifted relative to the solution phase value, indicating that H aggregates were formed in the solid state.^[15] On further performing UV/Vis absorption measurements for a HTA thin film deposited on quartz with similar initial optical densities (OD; Figure 2), no change of the intensity of absorption was observed for five months, which proved the high photostability of HTA.

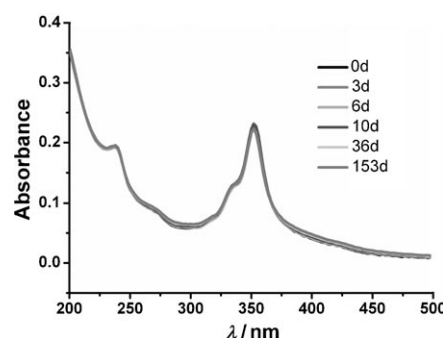


Figure 2. The photostability of HTA thin film deposited on quartz.

Further insight into the electronic properties of HTA was gained by cyclic voltammetry (CV) investigation at room temperature. We used a conventional three-electrode cell with a platinum wire counterelectrode, an Ag/AgCl reference electrode, and indium tin oxide (ITO)-coated glass working electrode in 0.1 M $\text{Bu}_4\text{NPF}_6/\text{CH}_3\text{CN}$ solution at room temperature. The CV measurements were acquired by means of an electrochemical method described in the literature.^[16] The CV plots displayed three-stage oxidation processes, and

reduction potentials below zero voltage could not be observed, as shown in Figure 3. However, this is an irreversible process, as the film degrades at high potential and dissolves

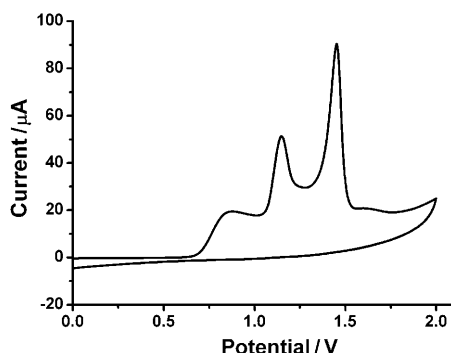


Figure 3. Cyclic voltammogram of HTA in 0.1 M Bu_4NPF_6 acetonitrile solution.

in solution. The first oxidation potential of HTA is 0.85 V versus Ag/AgCl, which is lower than that of PTA (1.12 V). The ionization potentials (E_{HOMO}) of π -conjugated systems can be estimated by using the equation $E_{\text{HOMO}} = -(4.40 + E_{\text{ox}})$ eV. The E_{ox} value is the onset potential for oxidation for HTA of 0.66 V, corresponding to the estimated E_{HOMO} of -5.06 eV. The HOMO value is close to the DFT-calculated value of -5.20 eV and higher than that of PTA (-5.33 eV) reported by us. In line with the DFT calculation of fused thiophenes, the HOMO energy increases while the energy gap decreases along with the increase of one thiophene unit. HTA has low-lying HOMO energy levels and large band gaps, which indicates that it is oxidatively more stable than pentacene ($E_{\text{HOMO}} = -4.60$ eV, $E_g = 2.21$ eV).^[17] Moreover, the HOMO level of HTA of -5.06 eV matches well with the work function of Au electrode (-5.10 eV), which results in less traps and reduced contact resistance and hence enhancement of the hole injection between the electrode and semiconductor layer in OTFTs.

To better understand the relationship between the film morphology and the mobility, thin films of HTA on different substrate surfaces were investigated by thin-film X-ray diffraction (XRD) and atomic force microscopy (AFM). The XRD profile of a vacuum-evaporated thin film of about 50 nm thickness deposited onto bare, *n*-octadecyltrichlorosilane (OTS)-treated and polystyrene (PS)-treated SiO_2/Si substrates at different T_{sub} values. In all films, the first-order reflection is very intense at $2\theta = 5.98^\circ$ (d spacing 1.476 nm) with the second-order diffraction peaks at $2\theta = 11.94^\circ$ (d spacing 0.740 nm). The first of these are coincident with the length of the molecules of HTA based on the extended molecular lengths optimized by ChemDraw 3D and calculated by Material Studio 3.0,^[16a] and the others are its second orders, indicating well-ordered, layered microstructures. It suggests that the molecules of HTA are standing near upright on the substrate along their long axis, with the π - π stacking direction parallel to the substrate with the current

flowing direction, and in that case the charge carriers would transport easily with high mobilities.^[18] The higher-order peaks became weaker until disappearance with increasing substrate temperatures (T_{sub}), which could be further confirmed by the following OTFT study. AFM images showed that the morphology of thin films strongly depended on the temperature of deposition. For the film on OTS/ SiO_2/Si or PS/ SiO_2/Si , at low temperature, large and consecutive grains were obtained, corresponding well with the high mobility. However, when the temperature of the substrate was increased further, the grains became small and the morphologies of the films became worse, which may be related to the drop in mobility.

OTFT devices were fabricated in a top-contact configuration with thin films of HTA as active organic semiconductor layers deposited onto SiO_2/Si , OTS/ SiO_2/Si , or PS/ SiO_2/Si . All the devices showed typical *p*-channel transistor characteristics under ambient conditions. The typical output and transfer characteristics of HTA on OTS/ SiO_2/Si at $T_{\text{sub}} = 20^\circ\text{C}$ are shown in Figure 4. The main parameters of device

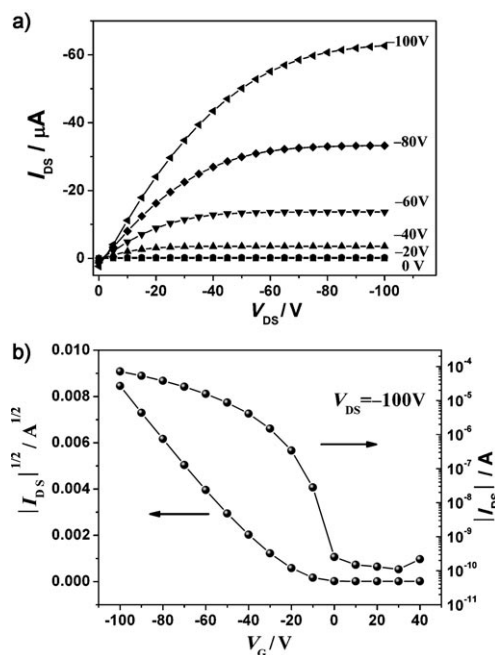


Figure 4. The output (a) and transfer (b) characteristics of OTFT devices based on HTA deposited on OTS-modified SiO_2/Si substrate at $T_{\text{sub}} = 20^\circ\text{C}$.

performance, that is, mobility (μ_{TFET}), threshold voltage (V_T), $I_{\text{on/off}}$ at different T_{sub} values are summarized (see Table S1 in the Supporting Information). For data analysis, it is clear that the OTFT performance strongly depends on both dielectric surface treatment and substrate temperature value.

Film morphology variations with T_{sub} may play an important role in mobility. The semiconductors based on HTA on untreated SiO_2/Si exhibit a mobility of $0.0022 \text{ cm}^2 \text{ V}^{-1} \text{ s}^{-1}$ at a substrate temperature of room temperature, which shows

a bit lower charge mobility than that of PTA ($0.0043 \text{ cm}^2 \text{ V}^{-1} \text{ s}^{-1}$). The experimental results are in good accordance with the calculated mobility trend by DFT calculations (hole transfer mobility: HTA $0.48 \text{ cm}^2 \text{ V}^{-1} \text{ s}^{-1}$, PTA $0.55 \text{ cm}^2 \text{ V}^{-1} \text{ s}^{-1}$) whereby PTA displayed quite good OTFT performance as *p*-type semiconductors of oligothienoacenes. For the same device geometry of semiconductor evaporated onto a SiO_2/Si substrate fabricated by our group, the grain sizes for PTA were on the order of $0.8 \times 2.5 \mu\text{m}^2$ at $T_{\text{sub}} = 80^\circ\text{C}$ with the best mobility of $0.045 \text{ cm}^2 \text{ V}^{-1} \text{ s}^{-1}$ while the grain sizes for HTA were much smaller at $T_{\text{sub}} = 100^\circ\text{C}$, on the order of $0.2 \times 0.2 \mu\text{m}^2$, with its best mobility of $0.0059 \text{ cm}^2 \text{ V}^{-1} \text{ s}^{-1}$. This difference of an order of magnitude in mobility is due to the difference in grain sizes observed by AFM images of the thin films when T_{sub} is changed, with smaller grains and poorer surface coverage noted for HTA than for PTA. It is demonstrated that the performances of field effect transistors are not enhanced largely by using HTA as semiconductor. Research interest has primarily focused on further extension of the conjugation, as in HTA, resulting in low mobility relative to PTA. Modification of the substrate with a self-assembled monolayer of OTS or PS was found to greatly improve the device performance relative to untreated SiO_2/Si substrates. The best performance of mobility ($0.06 \text{ cm}^2 \text{ V}^{-1} \text{ s}^{-1}$) and an on/off ratio of 7×10^5 were obtained at $T_{\text{sub}} = 20^\circ\text{C}$ on OTS-treated SiO_2/Si . A mobility of $0.03 \text{ cm}^2 \text{ V}^{-1} \text{ s}^{-1}$ and an on/off ratio of 2×10^3 were obtained at $T_{\text{sub}} = 20^\circ\text{C}$ on PS-treated SiO_2/Si .

In conclusion, we have synthesized a new linear six-thiophene-fused system of hexathienoacene and succeeded in its application for OTFTs. Our work actually affords the experimental results for the theoretical studies. We have demonstrated that further extension of the conjugation of oligothienoacenes does not increase the transistor performance, which would be valuable for the design and development of new organic semiconductors. The high mobility of $0.06 \text{ cm}^2 \text{ V}^{-1} \text{ s}^{-1}$ with current on/off ratio larger than 10^5 was obtained at room temperature on OTS-treated SiO_2/Si substrates.

Experimental Section

Synthesis of 3,6-bis-(thiophen-3-ylsulfanyl)-thieno[3,2-b]thiophene (**3**): To a solution of 3,6-dibromo-thieno[3,2-b]thiophene (2.98 g, 10 mmol) in anhydrous diethyl ether (100 mL) was added a 2.5 M solution of *n*BuLi in hexane (8 mL, 20 mmol) under a nitrogen atmosphere at -78°C . After stirring for 1 h at -78°C , to the resulting white suspension was added a solution of bis(3-thienyl) disulfide (4.60 g, 20 mmol) in anhydrous diethyl ether (10 mL). The mixture was allowed to warm and was stirred at room temperature for further 12 h after which time water (200 mL) was added. The aqueous phase was extracted twice with ether (100 mL) and dried over MgSO_4 . After removal of the solvent under reduced pressure, the residual was separated by chromatography on silica gel, using hexane as an eluent, to give the product (3.12 g, 85%) as a white solid. $^1\text{H NMR}$ (CDCl_3 , 400 MHz): $\delta = 7.01\text{--}7.02$ ppm (d, 2H, $J = 4.0$ Hz), 7.30–7.31 ppm (d, 6H, $J = 4.0$ Hz). $^{13}\text{C NMR}$ (CDCl_3 , 400 MHz): $\delta_{\text{C}} = 123.9$ (s), 126.5 (s), 126.6 (s), 127.9 (s), 128.6 (s), 130.3 (s), 140.5 ppm (s). MS: $m/z = 368$ (M^+ , 100). Elemental analysis (%) calcd for $\text{C}_{14}\text{H}_8\text{S}_6$: C 45.62, H 2.19; found: C 45.66, H 2.26.

Synthesis of hexathienoacene (HTA): To a stirred solution of sulfide **3** (2 g, 5.5 mmol) in anhydrous diethyl ether (100 mL) was added a 2.5 M solution of *n*BuLi in hexane (10 mL, 25 mmol) under a nitrogen atmosphere at -10°C . The mixture was stirred for 2 h and then added to a vigorously-stirred suspension of anhydrous CuCl_2 (3.38 g, 25 mmol) at 0°C in diethyl ether (30 mL). The mixture was allowed to warm and was stirred at room temperature for further 12 h. After removal of diethyl ether under reduced pressure, the residual was washed with dilute acid (5% HCl), water, methanol, then with acetone three times to remove the starting material. Further purification was carried out by sublimation three times to give HTA (120 mg, 6%) as yellow solids. HRMS (MALDI): m/z calcd for $[\text{C}_{14}\text{H}_8\text{S}_6]$: 363.8637; found: 363.8639. Elemental analysis (%) calcd for $\text{C}_{14}\text{H}_8\text{S}_6$: C 46.12, H 1.11, S 52.77; found: C 46.04, H 1.39, S 52.65.

Acknowledgements

The present research was financially supported by the National Natural Science Foundation of China (20825208, 60736004, 60911130231, 20721061, 20973184, 60901050), the National Major State Basic Research Development Program (2006CB806203, 2006CB932103, 2009CB623603), and the Chinese Academy of Sciences.

Keywords: acenes • conjugation • density functional calculations • sulfur • transistors

- a) W. P. Wu, Y. Q. Liu, D. B. Zhu, *Chem. Soc. Rev.* **2009**, 38, 3391–3400; b) C. Reese, M. Roberts, M.-M. Ling, Z. N. Bao, *Mater. Today* **2004**, 7, 20–27; c) Y. M. Sun, Y. Q. Liu, D. B. Zhu, *J. Mater. Chem.* **2005**, 15, 53–65; d) C. D. Dimitrakopoulos, P. R. L. Malenfant, *Adv. Mater.* **2002**, 14, 99–117; e) G. Horowitz, *Adv. Mater.* **1998**, 10, 365–377.
- J. E. Anthony, *Chem. Rev.* **2006**, 106, 5028–5048.
- a) A. R. Reddy, M. Bendikov, *Chem. Commun.* **2006**, 1179–1181; b) A. Maliakal, K. Raghavachari, H. Katz, E. Chandross, T. Siegrist, *Chem. Mater.* **2004**, 16, 4980–4986; c) P. Coppo, S. G. Yeates, *Adv. Mater.* **2005**, 17, 3001–3005.
- a) P. V. Schleyer, M. Manoharan, H. J. Jiao, F. Stahl, *Org. Lett.* **2001**, 3, 3643–3646; b) R. Mondal, R. M. Adhikari, B. K. Shah, D. C. Neckers, *Org. Lett.* **2007**, 9, 2505–2508.
- W. J. Bailey, C.-W. Liao, *J. Am. Chem. Soc.* **1955**, 77, 992–993.
- a) M. Bendikov, H. M. Duong, K. Starkey, K. N. Houk, E. A. Carter, F. Wudl, *J. Am. Chem. Soc.* **2004**, 126, 7416–7417; b) H. Angliker, E. Rommel, J. Wirz, *Chem. Phys. Lett.* **1982**, 87, 208.
- D. J. Gundlach, J. A. Nichols, L. Zhou, T. N. Jackson, *Appl. Phys. Lett.* **2002**, 80, 2925–2927.
- T. W. Kelley, L. D. Boardman, T. D. Dunbar, D. V. Muires, M. J. Pellerite, T. P. Smith, *J. Phys. Chem. B* **2003**, 107, 5877–5881.
- K. Xiao, Y. Liu, T. Qi, W. Zhang, F. Wang, J. Gao, W. Qiu, Y. Ma, G. Cui, S. Chen, X. Zhan, G. Yu, J. Qin, W. Hu, D. Zhu, *J. Am. Chem. Soc.* **2005**, 127, 13281–13286.
- a) M. Q. He, F. Zhang, *J. Org. Chem.* **2007**, 72, 442–451; b) K. Kudoh, T. Okamoto, S. Yamaguchi, *Organometallics* **2006**, 25, 2374–2377; c) T. Okamoto, K. Kudoh, A. Wakamiya, S. Yamaguchi, *Chem. Eur. J.* **2007**, 13, 548–556; d) X. N. Zhang, A. P. Côté, A. J. Matzger, *J. Am. Chem. Soc.* **2005**, 127, 10502–10503.
- H. Lumbroso, J. M. Catel, G. Le Coustumer, C. G. Andrieu, *J. Mol. Struct.* **1999**, 513, 201–218.
- L. S. Fuller, B. Iddon, K. A. Smith, *J. Chem. Soc. Perkin Trans. 1* **1997**, 3465–3470.
- a) Y. M. Sun, Y. Q. Ma, Y. Q. Liu, Y. Y. Lin, Z. Y. Wang, Y. Wang, C.-a. Di, K. Xiao, X. M. Chen, W. F. Qiu, B. Zhang, G. Yu, W. P. Hu, D. B. Zhu, *Adv. Funct. Mater.* **2006**, 16, 426–432; b) Y. Liu, Y.

- Wang, W. P. Wu, Y. Q. Liu, H. X. Xi, L. M. Wang, W. F. Qiu, K. Lu, C. Y. Du, G. Yu, *Adv. Funct. Mater.* **2009**, *19*, 772–778.
- [14] Y. X. Zhang, X. Cai, Y. Z. Bian, X. Y. Li, J. Z. Jiang, *J. Phys. Chem. C* **2008**, *112*, 5148–5159.
- [15] a) X. N. Zhang, J. P. Johnson, J. W. Kampf, A. J. Matzger, *Chem. Mater.* **2006**, *18*, 3470–3476; b) T. Kono, D. Kumaki, J.-i. Nishida, T. Sakanoue, M. Kakita, H. Tada, S. Tokito, Y. Yamashita, *Chem. Mater.* **2007**, *19*, 1218–1220; c) S. Tirapattur, M. Belletête, N. Drolet, M. Leclerc, G. Durocher, *Chem. Phys. Lett.* **2003**, *370*, 799–804.
- [16] a) X. K. Gao, W. P. Wu, Y. Q. Liu, S. B. Jiao, W. F. Qiu, G. Yu, L. M. Wang, D. B. Zhu, *J. Mater. Chem.* **2007**, *17*, 736–743; b) J. L. Brédas, R. Silbey, D. S. Boudreaux, R. R. Chance, *J. Am. Chem. Soc.* **1983**, *105*, 6555–6561; c) R. Cernini, X. Li, W. C. Spencer, A. B. Holmes, S. C. Moratti, R. H. Friend, *Synth. Met.* **1997**, *84*, 359–360; d) H. Tian, J. Shi, D. Yan, L. Wang, Y. Geng, F. Wang, *Adv. Mater.* **2006**, *18*, 2149–2152; e) M. Thelakkat, H.-W. Schmidt, *Adv. Mater.* **1998**, *10*, 219–223.
- [17] H. Meng, M. Bendikov, G. Mitchell, R. Helgeson, F. Wudl, Z. Bao, T. Siegrist, C. Kloc, C. H. Chen, *Adv. Mater.* **2003**, *15*, 1090–1093.
- [18] a) L. S. Miguel, W. W. Porter III, A. Matzger, *Org. Lett.* **2007**, *9*, 1005–1008; b) Y. Wu, Y. Li, S. Gardner, B. S. Ong, *J. Am. Chem. Soc.* **2005**, *127*, 614–618; c) H. Meng, Z. Bao, A. J. Lovinger, B. C. Wang, A. M. Mujsce, *J. Am. Chem. Soc.* **2001**, *123*, 9214–9215; d) F. Valiyev, W.-S. Hu, H.-Y. Chen, M.-Y. Kuo, I. Chao, Y.-T. Tao, *Chem. Mater.* **2007**, *19*, 3018–3026.

Received: January 1, 2010
Published online: May 17, 2010